A proteomic approach identifies SAFB-like transcription modulator (SLTM) as a bidirectional regulator of GLI family zinc finger transcription factors

Received for publication, December 5, 2018, and in revised form, February 11, 2019 Published, Papers in Press, February 19, 2019, DOI 10.1074/jbc.RA118.007018

Zilai Zhang[‡1], **Xiaoming Zhan**[‡§1], **Bongwoo Kim**[‡1], **and Jiang Wu**[‡2]

From the [‡]*Department of Physiology and* [§]*Center for the Genetics of Host Defense, University of Texas Southwestern Medical Center, Dallas, Texas 75390*

Edited by Joel M. Gottesfeld

In Sonic hedgehog (SHH) signaling, GLI family zinc finger (GLI)-mediated diverse gene transcription outcomes are strictly regulated and are important for SHH function in both development and disease. However, how the GLI factors differentially regulate transcription in response to variable SHH activities is incompletely understood. Here, using a newly generated, tagged *Gli3* knock-in mouse (*Gli3*^{TAP}), we performed proteomic analyses and identified the chromatin-associated SAFB-like transcription modulator (SLTM) as a GLI-interacting protein that context-dependently regulates GLI activities. Using immunoprecipitation and immunoblotting, RT-quantitative PCR, and ChIP assays, we show that SLTM interacts with all three GLI proteins and that its cellular levels are regulated by SHH. We also found that SLTM enhances GLI3 binding to chromatin and increases GLI3 repressor (GLI3R) form protein levels. In a GLI3-dependent manner, SLTM promoted the formation of a repressive chromatin environment and functioned as a GLI3 co-repressor. In the absence of GLI3 or in the presence of low GLI3 levels, SLTM co-activated GLI activator (GLIA)-mediated target gene activation and cell differentiation. Moreover, *in vivo Sltm* deletion generated through CRISPR/Cas9-mediated gene editing caused perinatal lethality and SHH-related abnormal ventral neural tube phenotypes. We conclude that SLTM regulates GLI factor binding to chromatin and contributes to the transcriptional outcomes of SHH signaling via a novel molecular mechanism.

Sonic hedgehog (SHH)[3] signaling plays important roles during development and in cancer growth. Mutations that affect the SHH pathway cause severe birth defects and cancers (1–5). SHH signaling mediated through Patched (Ptch1) and Smoothened (Smo) controls target gene expression by differentially regulating activities of the GLI family of zinc finger transcription factors (1, 3, 6). GLI family transcription factors carry out the diverse transcription outcomes of SHH signaling. In the absence of SHH, full-length GLI3 (GLI3FL) can be proteolyzed, and the C-terminal truncated protein GLI3R functions as the main repressor of expression of SHH target genes (7). In the presence of SHH, SHH signaling activates GLI1/2 proteins and inhibits GLI3 proteolysis. GLI1 and GLI2 are the main transcription activators that mediate SHH-induced transcription. The balance of protein levels and activities of GLI activator (GLIA) and GLI repressor (GLIR) forms determines transcription outcomes in specific cell types during specific developmental stages (8–10).

How GLI factors differentially regulate transcription in response to different SHH activities during development is under active investigation. GLI proteins share a conserved zinc finger domain containing five zinc fingers, which is responsible for binding to DNA and may also interact with co-factors (11). The three GLI family members could bind to the same consensus DNA sequences but exert different transcription outcomes (1, 10, 12, 13). The N- and C-terminal regions of GLI proteins are more diverse and display repressing or activating functions, likely through interactions with different proteins. Interestingly, some proteins could interact with all three GLI proteins and exert context-dependent opposite functions in SHH signaling (14, 15).

SHH regulates GLI proteins by influencing protein expression, processing, localization, and degradation. GLI transcription activities are also regulated by post-translational modifications such as phosphorylation, acetylation, ubiquitination, and sumoylation (10, 12, 16). Suppressor of fused homolog (SUFU) is a main negative regulator of SHH signaling, which regulates GLI activities at several levels. Without the SHH signal, SUFU binds to GLI3 and the complex is recruited to primary cilia, leading to the efficient processing of GLI3FL into GLI3R (17, 18). SHH activation leads to the dissociation of SUFU from

This work was supported by funds from the March of Dimes Foundation, Welch Foundation Grant I-1940–20170325 (to J. W.), and National Institutes of Health Grants R01NS09606 and R21NS104596 (to J. W.). The authors declare that they have no conflicts of interest with the contents of this article. The content is solely the responsibility of the authors and does not necessarily represent the official views of the National Institutes of Health.

This article contains Table S1.

[1] These authors contributed equally to this work.

[2] To whom correspondence should be addressed: Dept. of Physiology, UT Southwestern Medical Center, 5323 Harry Hines Blvd., Dallas, TX 75390-9040. Tel.: 214-648-1824; E-mail: jiang9.wu@utsouthwestern.edu.

[3] The abbreviations used are: SHH, Sonic hedgehog; SLTM, SAFB-like transcription modulator; GLIA, GLI activator; GLIR, GLI repressor; GLI3FL, full-length GLI3; TAP, tandem affinity purification; qPCR, quantitative PCR; IP, immunoprecipitation; MEF, mouse embryonic fibroblast; H3K27me3, histone H3 lysine 27 trimethylation; H3K4me3, histone H3 lysine 4 trimethylation; H3K9me2, histone H3 lysine 9 dimethylation; ES cell, embryonic stem cell; E, embryonic day; HA, hemagglutinin; NP-40, Nonidet P-40; RIPA, radioimmune precipitation assay; GAPDH, glyceraldehyde-3-phosphate dehydrogenase; ANOVA, analysis of variance.

GLI3FL, allowing its translocation to the nucleus, where it is phosphorylated, destabilized, and converted to a transcriptional activator (GLI3A) (19–21). In addition, SUFU negatively regulates GLIA by binding to GLI1/2 and sequestering them in the cytoplasm (20–22). SUFU has also been shown to function in the nucleus to repress GLIA activities (23, 24). Primary cilia play context-dependent opposite roles in regulating GLI activities. Primary cilia are not only required for GLI3 processing to produce GLIR, but it also is required for GLIA dissociation from SUFU and pathway activation (14, 25).

In the nucleus, the mechanism regulating GLI activities is emerging. We and others have shown that distinct transcription co-factor complexes are formed with GLIR or GLIA to produce different transcription outcomes (10, 26). Chromatin-remodeling BAF complexes interact with all three GLI proteins; depending on context, BAF may repress or activate basal and signaling-induced target gene transcription (15, 27). In basal conditions, the SHH target genes labeled by bivalent chromatin domains are repressed by an epigenetic network that involves BAF complexes and PRC2 complexes. In response to SHH stimulation, there is an exchange from GLIR to GLIA at the gene regulatory regions, resulting in a switch from co-repressor complexes to co-activator complexes including BRG1, JMJD3, and MLL (26). GLI proteins have also been shown to interact with other chromatin regulators, such as HDACs and CBP (28, 29). Thus, understanding of the GLI-interacting proteins will provide insights into the mechanisms underlying the GLI-mediated diverse transcription activities and SHH-related birth defects and childhood diseases.

An obstacle to identification of GLI-interacting proteins has been the lack of suitable anti-GLI antibodies. To overcome this, we engineered the *Gli3* locus and generated a tagged GLI3 knock-in mouse. Using this mouse, we affinity-purified GLI3-interacting nuclear proteins and identified SAFB-like transcription modulator (SLTM) as a GLI-interacting protein. We showed that SLTM interacts with all three GLI proteins. SLTM enhances GLI3 binding to chromatin and increases GLI3R protein levels. In a GLI3-dependent manner, SLTM promotes the formation of a repressive chromatin environment. In the absence of GLI3 or in the presence of low levels of GLI3, SLTM functions to co-activate GLIA-mediated target gene activation and cell differentiation. Therefore, SLTM regulates GLI factor binding to chromatin and contributes to the precise transcription outcomes of SHH signaling with a novel mechanism.

Results

Generation of $Gli3^{TAP}$ knock-in mice

To identify GLI3-interacting proteins, we engineered the mouse *Gli3* locus and knocked in a tandem affinity purification (TAP) tag using homologous recombination. The TAP tag contains a protein A tag and an HA tag separated by a Tev protease cleavage site (Fig. 1*A*). Correctly recombined embryonic stem cell (ES cell) clones were identified by PCR (Fig. 1*B*) and Southern blotting (Fig. 1*C*). The $Gli3^{TAP\text{-}neo}$ mouse line was generated through germ line transmission. The neomycin expression cassette was then removed by crossing to a Cre transgene. The resulting $Gli3^{TAP/+}$ heterozygous and $Gli3^{TAP/TAP}$ homozygous mice are normal and fertile, indicating the normal function of the protein encoded by the $Gli3^{TAP}$ allele. In the $Gli3^{TAP/+}$ heterozygous telencephalon, TAP-GLI3 and WT GLI3 proteins were expressed and processed at comparable levels (Fig. 1*D*). To further determine whether the TAP tag alters the function of GLI3, we crossed $Gli3^{TAP/TAP}$ mice to mice with a *Gli3-null* allele. $Gli3^{TAP/-}$ mice grow normally but have one extra first digit (Fig. 1*E*), a phenotype similar to $Gli3^{+/-}$ extra toe mice (30). Therefore, TAP-GLI3 protein likely functions similarly to WT GLI3 and can be used to study GLI3 protein properties.

Affinity purification of TAP-GLI3 and associated proteins

Previously, we have shown that GLI3 interacts with a chromatin remodeler BRG1 and mediates recruitment of BRG1 to the regulatory regions of SHH/GLI target genes during development (15). Using E13.5 $Gli3^{TAP/TAP}$ telencephalons, where GLI3 expression levels are high, we immunoprecipitated endogenous TAP-GLI3 with IgG beads, which could bind to the Protein A fragment in the TAP tag; endogenous BRG1 was enriched in this precipitate (Fig. 2*A*). ChIP analyses with IgG beads of chromatin from E13.5 telencephalons also showed binding of TAP-GLI3 at the regulatory regions of SHH/GLI target genes (Fig. 2*B*). These results further confirmed that the addition of the TAP tag did not disrupt the molecular properties of GLI3.

We then performed affinity purification of GLI3-associated complexes and identified GLI3-interacting proteins with MS. E13.5 telencephalons were used to prepare nuclear extracts. Due to the difficulty of releasing GLI3 proteins by Tev digestion from the beads after the first step of purification, we performed a one-step affinity purification using IgG-Sepharose beads (Fig. 2*C*). Western blotting showed a significant enrichment of TAP-GLI3 (GLI3FL and GLI3R) in the elution fractions (Fig. 2*D*). WT telencephalons were used as a negative control. The proteins identified from the TAP-GLI3–expressing telencephalons but not the WT tissues were candidate GLI3-interacting proteins. Forty specific proteins were identified, including many proteins with known or predicted functions in transcription regulation (Table S1). Importantly, among these hits, GLI3 was identified with the greatest number of recovered peptides. The known GLI3-interacting proteins KIF7 (Cos2 homolog) (31) and SUFU ranked number 3 and 5, respectively (Table S1 and Fig. 2*E*). The identification of GLI3 (Fig. 2*F*) and these known GLI3-interacting proteins validates our purification approach. Notably, one of the top hits is SLTM, with 14 peptides recovered (Fig. 2, *E* and *F*). SLTM is a member of the SAF-box protein family; other family members often function as transcription co-repressors or co-activators through diverse and context-dependent mechanisms (32–34). Thus, it is possible that SLTM regulates GLI3 functions.

SLTM interacts with GLI proteins

To understand the interactions between SLTM and GLI proteins, we expressed both GLI3 and HA-SLTM in SHH-responsive NIH3T3 cells. Immunoprecipitation (IP) with anti-GLI3 antibodies co-purified GLI3 and SLTM (Fig. 3*A*). To determine which region of the GLI3 protein interacts with SLTM, we per-

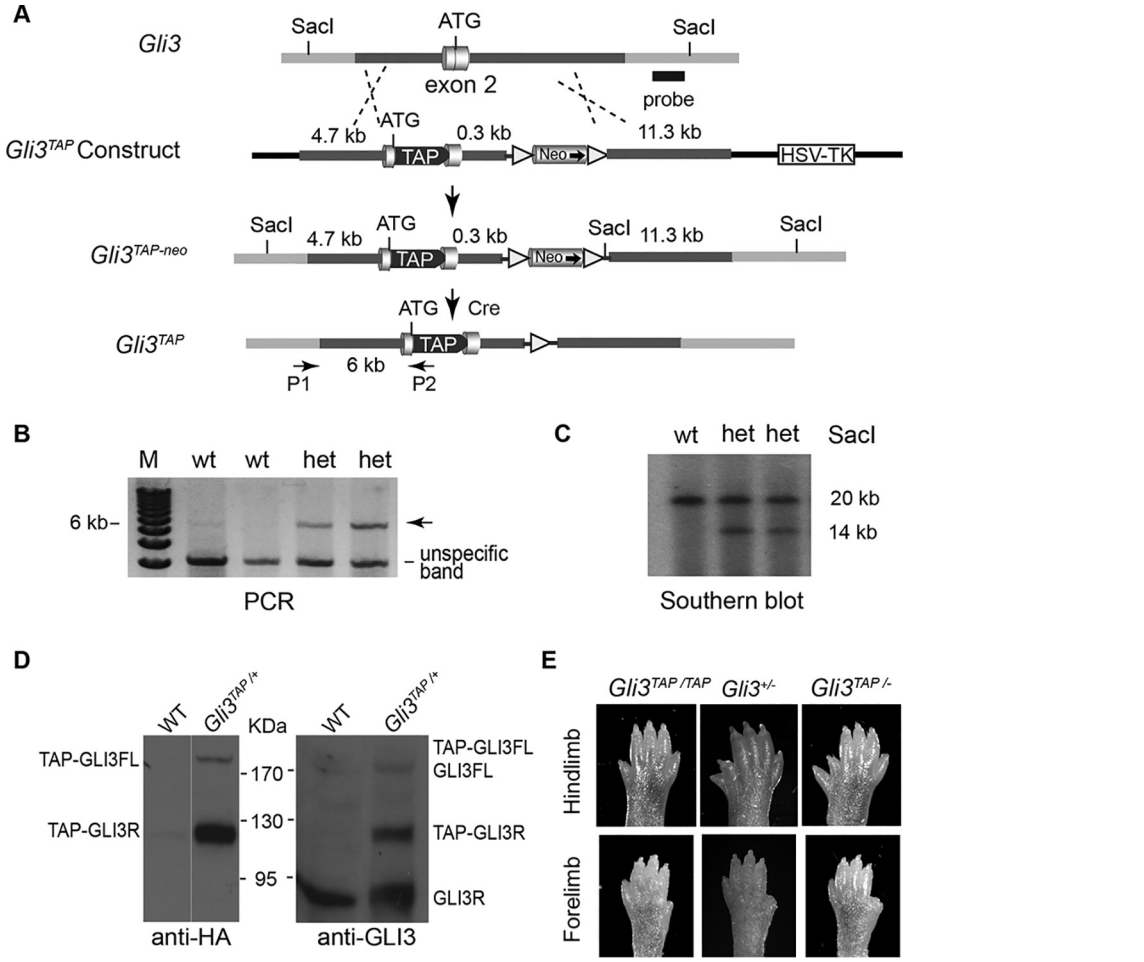

Figure 1. Generation of *Gli3*^{TAP} knock-in mice. *A*, structures of the *Gli3* allele, the *Gli3*^{TAP} knock-in construct, the *Gli3*$^{TAP\text{-}neo}$ allele, and the final *Gli3*^{TAP} allele. *B*, genotyping of correctly recombined *Gli3*^{TAP} allele in ES cells using primers P1 and P2 indicated in *A*. *C*, the correctly engineered allele was also confirmed by Southern blotting using an external probe on the 3′ side. *D*, TAP-GLI3 expression analyzed in E13.5 *Gli3*$^{TAP/+}$ telencephalons using Western blotting with anti-HA or anti-GLI3 antibodies. *E*, digit phenotypes of *Gli3*$^{TAP/TAP}$ homozygous mice, *Gli3*$^{+/-}$ extra toe mice, and *Gli3*$^{TAP/-}$ mice.

formed co-IP experiments using HA-tagged GLI3 fragments and FLAG-SLTM. We observed interactions between SLTM and GLI3R, the N-terminal domain (GLI3N) and to a lesser degree the C-terminal domain (GLI3C), but not the zinc finger domain (Fig. 3*B*). We also examined the interactions between both GLI1 and GLI2 proteins with SLTM. SLTM co-immunoprecipitated with all three GLI proteins from NIH3T3 cell extracts (Fig. 3*C*).

SLTM represses SHH/GLI target gene expression

The transcriptional outcome of SHH signaling is mainly determined by the balance between GLIA and GLIR activities. In primary mouse embryonic fibroblast (MEF) cells and similarly NIH3T3 cells, under basal conditions, GLI3 represses the expression of target genes, such as *Gli1* and *Ptch1*. SHH treatment or introduction of exogenous GLI1 induces the activation of these genes. Because SAFB family proteins often function as repressors, we reasoned that SLTM likely facilitates the repression of SHH/GLI target genes. To determine the function of SLTM, we generated *Sltm*$^{-/-}$ mice using the CRISPR/Cas9 method. The second coding exon was targeted, and a DNA fragment encoding GFP was inserted in frame (Fig. 4, *A* and *B*). SLTM proteins were not produced in *Sltm*$^{-/-}$ MEF cells (Fig. 4*C*). Therefore, it is likely a null allele. GFP expression in *Sltm*$^{+/-}$ and *Sltm*$^{-/-}$ embryos indicated that SLTM is ubiquitously expressed (Fig. 4*D*). *Sltm*$^{-/-}$ mice die soon after birth without obvious growth defects (data not shown).

Sltm deletion in MEF cells led to a de-repression of SHH target genes under basal conditions. SHH target genes *Gli1* and *Ptch1* were present at higher levels in *Sltm*$^{-/-}$ MEFs than in WT control cells (Fig. 4*E*). SLTM is not a general repressor because Wnt target genes *Axin2* and *C-Myc* were not de-repressed in *Sltm*$^{-/-}$ MEFs (Fig. 4*E*). Furthermore, overexpression of SLTM in NIH3T3 cells significantly repressed the SHH-induced target gene expression (Fig. 4*F*). Overexpression of SLTM also inhibited endogenous *Gli1* expression induced by exogenous GLI1 activator (Fig. 4*G*). Therefore, SLTM is required for repression of SHH/GLI target genes, such as *Gli1* and *Ptch1*, whereas excess SLTM represses SHH-induced expression of these genes.

SLTM enhances GLI3 binding to chromatin and is regulated by SHH

SHH signaling activation inhibits GLI3 processing and leads to the degradation of GLI3 proteins and departure of GLI3R from the chromatin and nucleus. To determine how SLTM

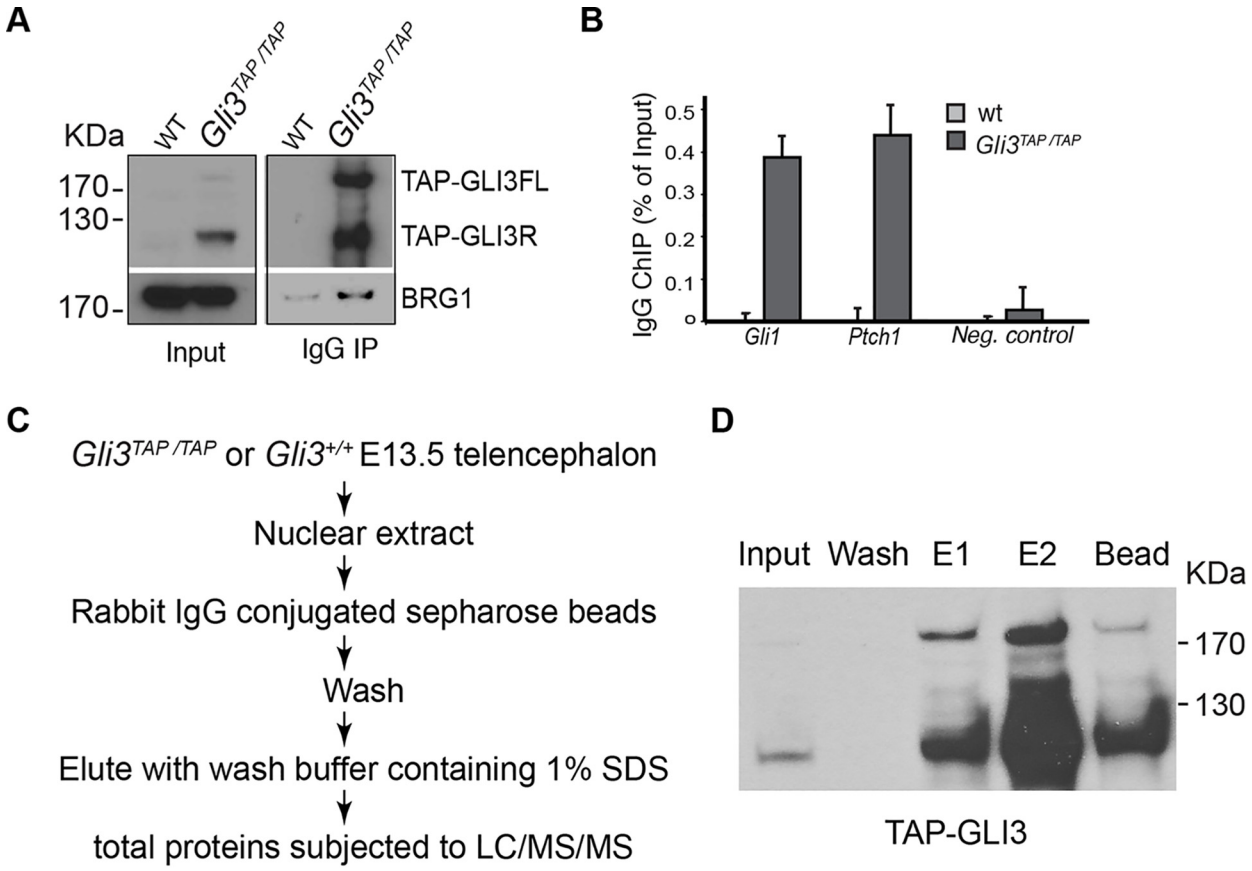

E

Top hits identified from TAP-GLI3 mass spectrometry.

Protein	Description	Length (aa)	Peptide #	MIC Sln
B2RUG4	GLI3	1583	36	4.31E-06
B9EI57	SAFB-like, transcription modulator (Sltm)	1031	14	2.60E-06
B7ZNG0	KIF7 (Cos2 homolog)	1348	7	1.07E-07
Q8R3P6	C15orf44 homolog	515	7	1.74E-08
Q3U0Z8	Suppressor of fused homolog (Sufu)	485	6	6.04E-07

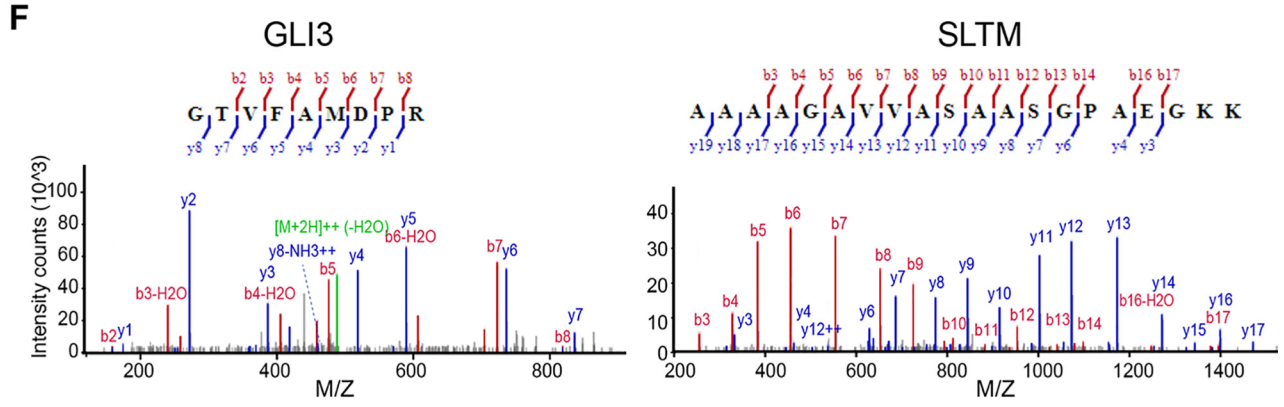

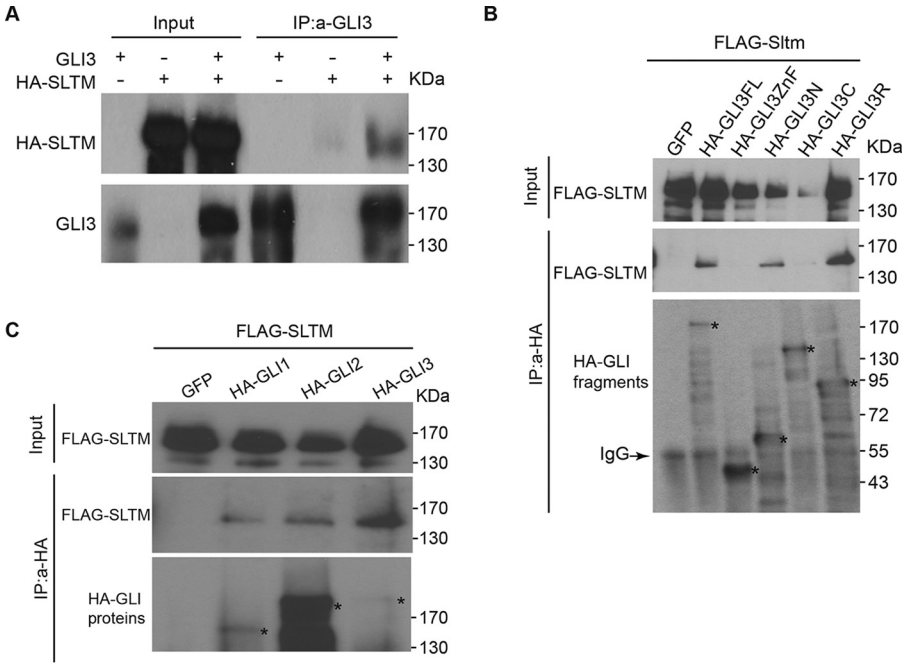

Figure 3. SLTM interacts with GLI proteins. *A*, extracts of NIH3T3 cells expressing HA-SLTM and GLI3 were immunoprecipitated with anti-GLI3 antibodies and Western blotted with antibodies against GLI3 and SLTM. HA-SLTM co-immunoprecipitated with GLI3. *B*, SLTM interacts with GLI3R and GLI3 N-terminal domain (GLI3N), but not the zinc finger (*ZnF*) region of GLI3. NIH3T3 cells expressing FLAG-SLTM and HA-tagged GLI3 fragments were immunoprecipitated with anti-HA antibody and analyzed by Western blotting with antibodies against FLAG or HA. *, HA-tagged GLI3 fragments. *C*, SLTM interacts with GLI1 and GLI2, as shown by expression of the indicated tagged proteins in NIH3T3 cells followed by immunoprecipitation and Western blotting. *, HA-tagged GLI proteins. Shown are representative results from at least three independent experiments.

regulates GLI3 repressor activities, we examined the SLTM and GLI3 protein levels in NIH3T3 cells that were treated with SHH and overexpressed increasing amounts of SLTM. SHH treatment led to decreased endogenous SLTM levels as well as lower GLI3R levels (Fig. 5*A*). Overexpression of SLTM in the presence of SHH increased GLI3 protein levels and repressed SHH-induced GLI1 expression in an SLTM dose-dependent manner (Fig. 5*A*). These results suggest that SLTM protein level is regulated by SHH, and it positively regulates GLI3 protein levels.

In NIH3T3 cells that express exogenous SLTM, SLTM was localized in the nucleus and was enriched in the chromatin fraction (Fig. 5*B*). Interestingly, overexpression of SLTM significantly increased the level of GLI3R in the chromatin fraction relative to overexpressing control proteins, but levels of the full-length GLI3 were similar in control cells and cells that overexpressed SLTM (Fig. 5*B*). The increase of GLI3R in the chromatin fraction in the presence of excess SLTM suggests that GLI3R binding to the regulatory regions of its target genes was increased. ChIP analyses indicated that SLTM binds to the regulatory regions of SHH target genes such as *Gli1* and that the binding was attenuated upon SHH treatment (Fig. 5*C*). Overexpression of SLTM increased GLI3 binding to the *Gli1* regulatory region (Fig. 5*D*). In contrast, in $Sltm^{-/-}$ MEFs, binding of GLI3 to the *Gli1* regulatory region was significantly reduced compared with levels in control cells (Fig. 5*E*). These results suggest that SLTM enhances GLI3 retention in the chromatin fraction.

SLTM facilitates the formation of a repressive chromatin environment at the Gli1 locus

Previously, we showed that GLI3-mediated repression of SHH target genes is associated with a repressive chromatin environment (15, 26). Under basal conditions, SHH target genes are marked by a bivalent domain containing a repressive H3K27me3 and an active H3K4me3 mark. Histone H3 lysine 27 methyltransferase complex PRC2 maintains the H3K27me3 mark repressing the expression of the SHH target genes. SHH activation induces an epigenetic switch. GLI3R is displaced from SHH target gene promoters, and GLIA binds and recruits H3K27me3 demethylase Jmjd3 to remove H3K27me3 marks and activate target gene expression.

In a recent proteomic study, SLTM was shown to interact with PRC2 (35); therefore, we examined whether an excess of SLTM would alter H3K27me3 levels in SHH target gene regulatory regions. In NIH3T3 cells, overexpression of SLTM significantly increased the H3K27me3 levels at the *Gli1* locus (Fig. 6*A*). Consistently, overexpression of SLTM also increased local PRC2 levels, as shown by the increase in levels of the PRC2 subunit SUZ12 in the *Gli1* regulatory regions (Fig. 6*B*). Interestingly, we also observed another repressive

Figure 2. Affinity purification of TAP-GLI3 and associated proteins. *A*, immunoprecipitation of TAP-GLI3 from E13.5 $Gli3^{TAP/TAP}$ telencephalons with IgG also pulled down BRG1. WT telencephalons were used as a negative control. *B*, ChIP-qPCR analyses of TAP-GLI3 binding to SHH/GLI target gene regulatory regions in E13.5 $Gli3^{TAP/TAP}$ knock-in telencephalons using IgG (*black bars*). WT telencephalons were used as a negative control (*gray bars*) ($n = 3$). *C*, procedures of affinity purification of TAP-GLI3 and interacting proteins. *D*, Western blot analysis of TAP-GLI3 proteins in different fractions during purification shows the enrichment of TAP-GLI3 after affinity purification. *E1*, elution fraction 1; *E2*, elution fraction 2. *E*, top protein hits identified by MS in TAP-GLI3 affinity purification. *F*, representative MS/MS fragment ion spectrum with peak assignments for GLI3 and SLTM.

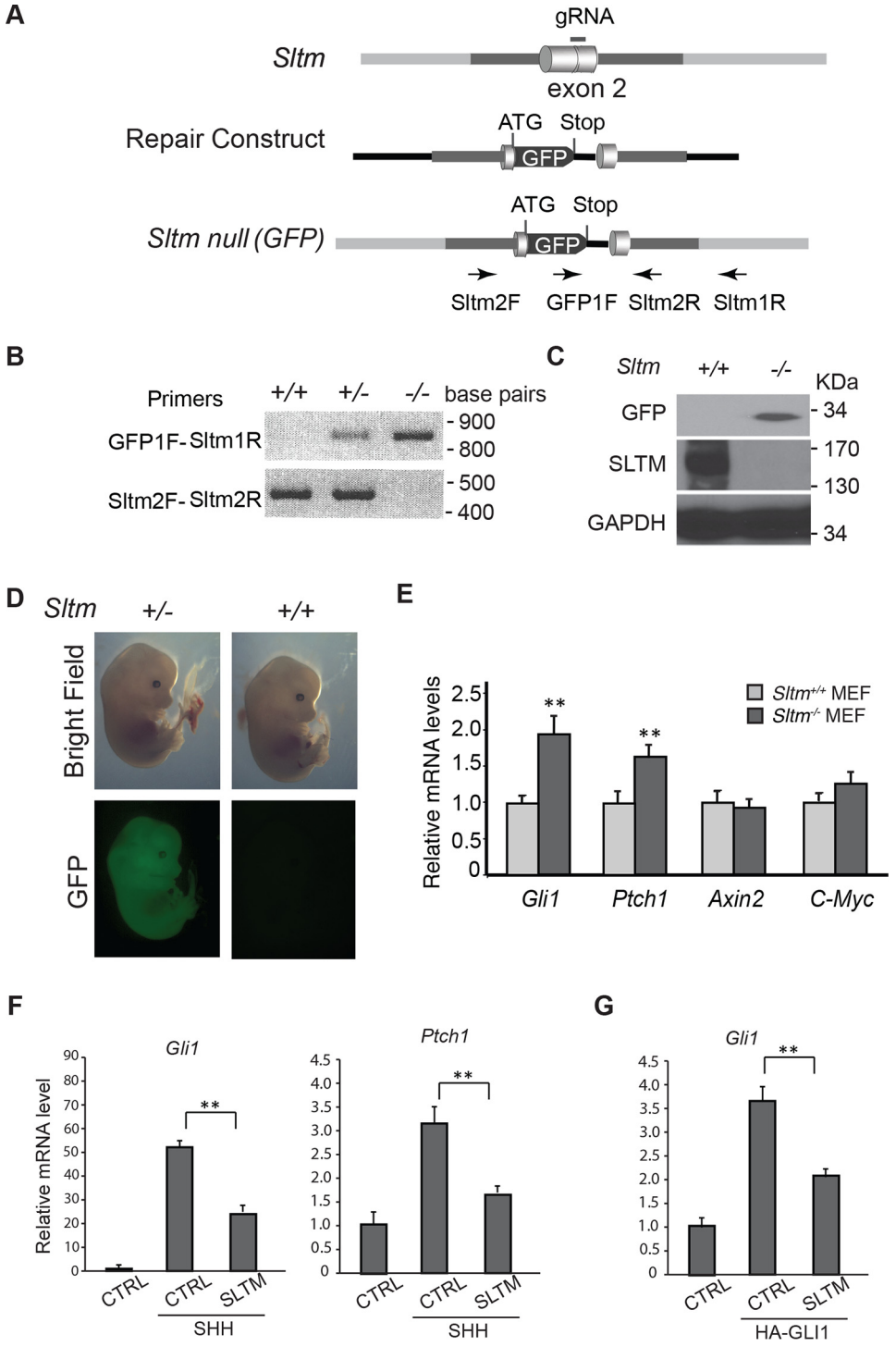

Figure 4. SLTM represses SHH/GLI target genes expression. *A*, *Sltm* null allele was generated using CRISPR-Cas9. The genomic structures of WT and mutant *Sltm* alleles are shown. A GFP gene was inserted into the *Sltm* null allele. *B*, PCR was used to compare genotypes of WT (+/+), $Sltm^{+/-}$ (+/−), and $Sltm^{-/-}$ embryos in the region of the *Sltm* allele. *C*, as shown by Western blotting of extracts from WT and $Sltm^{-/-}$ MEFs, SLTM was not expressed in $Sltm^{-/-}$ MEFs, and GFP was. *D*, ubiquitous expression GFP driven by the *Sltm* promoter in E13.5 $Sltm^{+/-}$ embryos. *E*, basal expression of SHH target genes *Gli1* and *Ptch1* in $Sltm^{-/-}$ MEFs (*black bars*, $n = 3$) and WT (*gray bars*, $n = 3$), as indicated by RT-qPCR. **, $p < 0.01$. *F*, overexpression of SLTM but not the empty vector control in SHH-treated NIH3T3 cells repressed SHH-induced expression of *Gli1* and *Ptch1* as measured by RT-qPCR. **, $p < 0.01$. *G*, overexpression of SLTM in NIH3T3 cells inhibited *Gli1* expression induced by exogenous Gli1 as measured by RT-qPCR. **, $p < 0.01$. RT-qPCR graphics in *F* and *G* are representative of at least three experiments performed in triplicate ($n = 3$). Significance was determined by Student's *t* test. *Error bars*, S.D.

histone mark, H3K9me2, in the regulatory region, and SLTM overexpression led to an increase in this mark (Fig. 6*C*). Histone H3 ChIP-qPCR was used as a control; similar levels of nucleosome occupancy were observed in control cells and in cells in which SLTM was overexpressed (Fig. 6*D*). Thus, SLTM may repress SHH target genes by both enhancing GLI3 binding and facilitating the generation of a repressive chromatin environment.

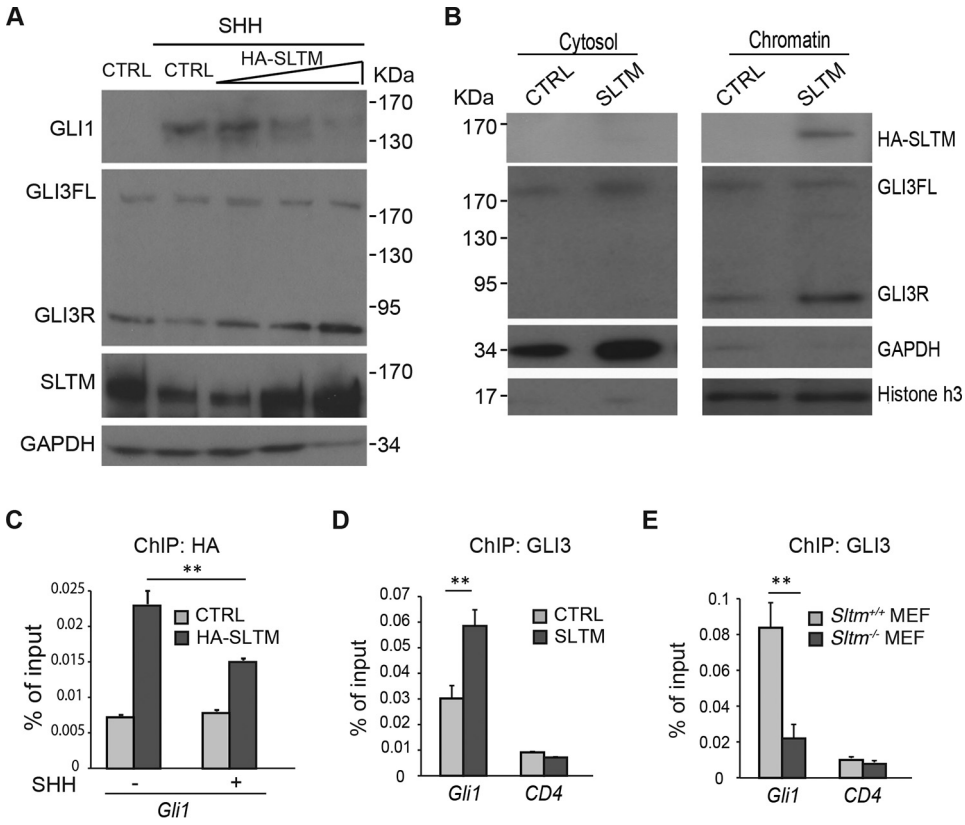

Figure 5. SLTM enhances GLI3 binding to chromatin. *A*, levels of SLTM and GLI were evaluated by Western blotting in NIH3T3 cells that overexpressed different amounts of SLTM; cells were stimulated with SHH or left unstimulated. *B*, NIH3T3 cells overexpressing SLTM or transfected with a control vector were fractionated. SLTM, GLI3FL, and GLIR in the cytoplasmic fraction and in chromatin were detected by Western blotting. *C*, SLTM binding to the *Gli1* regulatory region in control (*gray*) and SLTM-expressing (*black*) NIH3T3 cells was measured by ChIP-qPCR. *D*, binding of GLI3 to the *Gli1* regulatory region in control (*gray*) and SLTM-expressing (*black*) NIH3T3 cells was measured by ChIP-qPCR. *E*, ChIP-qPCR analyses of GLI3 binding to the *Gli1* regulatory region in WT or $Sltm^{-/-}$ MEFs. ChIP-qPCR graphics in *C–E* are representative of at least three experiments performed in triplicate ($n = 3$). Significance was determined by Student's *t* test. **, $p < 0.01$. *Error bars*, S.D.

SLTM activates SHH/GLI target genes in the absence of GLI3

Our experiments indicate that SLTM facilitates the binding of GLI3R to specific SHH target gene regulatory regions and helps to generate and maintain a repressive chromatin environment. Because GLI3R is the major repressor in SHH signaling, we examined whether the repressive function of SLTM on SHH signaling is GLI3-dependent. Surprisingly, in $Gli3^{-/-}$ MEFs, instead of repressing target gene expression as it did in the WT cells (Fig. 4*F*), excess SLTM enhanced the expression of SHH/GLI target genes in response to SHH stimulation. SHH-induced *Gli1* and *Ptch1* expression were both higher upon SLTM overexpression in $Gli3^{-/-}$ MEFs (Fig. 7*A*).

To determine whether this effect of SLTM on SHH target gene expression was due to the absence of GLI3, we reintroduced GLI3 into $Gli3^{-/-}$ MEFs. Modest lentivirus-expressed levels of GLI3R diminished the activator effect of SLTM on target gene expression (Fig. 7*B*), suggesting that the absence of GLI3 switched SLTM from a repressor to an activator. Because SLTM also interacts with GLI activators, albeit with a lower affinity (Fig. 3*C*), it is possible that in the absence of GLI3 or in the presence of low levels of GLI3R, SLTM could facilitate the binding of GLI2 to chromatin. Indeed, although excess SLTM did not enhance GLI2 binding to the *Gli1* regulatory regions in WT MEFs, in $Gli3^{-/-}$ cells, SLTM significantly increased GLI2 binding to the regulatory regions (Fig. 7*C*). These results suggest that the relative levels or activities of GLIA and GLIR determine whether SLTM functions as an activator or a repressor of SHH target genes.

Because SLTM positively regulated GLI3R levels, we examined GLI3 levels in $Sltm^{-/-}$ MEFs. In $Sltm^{-/-}$ MEFs, levels of GLI3R were lower than in WT cells and were similar to the low GLI3 levels observed in WT cells upon SHH stimulation (Fig. 7*D*). Interestingly, In $Sltm^{-/-}$ MEFs, SHH-induced *Gli1* activation was impaired (Fig. 7*E*), suggesting that SLTM functions as a co-activator for GLIA. The low GLI3R levels in SHH-stimulated cells may be responsible for switching SLTM from a repressor to an activator. The repressor function of SLTM observed in unstimulated NIH3T3 and MEF cells and in stimulated NIH3T3 cells in which SLTM is overexpressed depends on the presence of high GLI3 levels. Thus, in the absence of GLI3 or when GLI3 levels are low, SLTM functions as an activator of SHH target genes.

SLTM deletion leads to abnormal expression of ventral neural tube markers

To determine whether SLTM regulates SHH-dependent developmental processes, we examined $Sltm^{-/-}$ embryos for expression of ventral neural tube markers. As a morphogen, SHH is important for neural tube patterning and neural progenitor specification. In developing neural tube, SHH/GLIA are

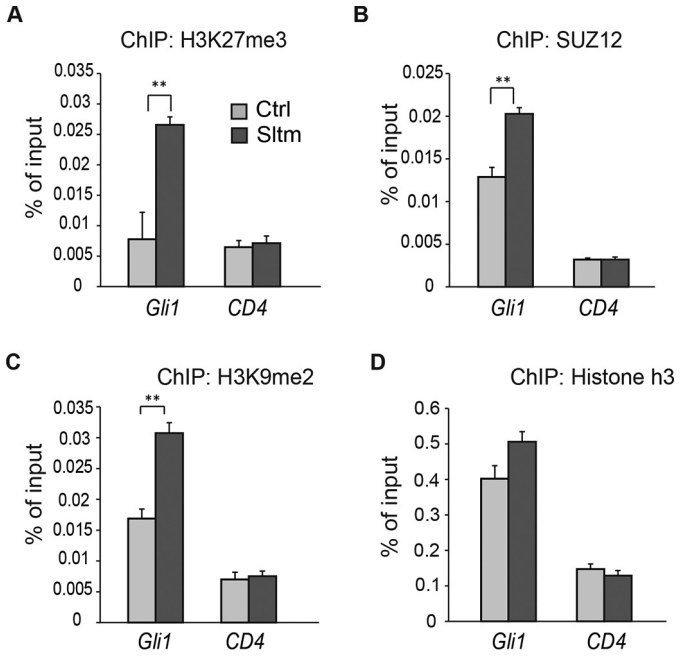

Figure 6. SLTM facilitates the formation of a repressive chromatin environment at the *Gli1* locus. ChIP-qPCR analyses were performed on extracts of control (*gray*) and SLTM-expressing (*black*) NIH3T3 cells using antibodies to H3K27me3 (*A*), SUZ12 (*B*), H3K9me2 (*C*), and histone H3 (*D*) in the *Gli1* locus. Histone H3 occupancy was used as a control. ChIP-qPCR graphics are representative of at least three experiments performed in triplicate ($n = 3$). Significance was determined by Student's *t* test. **, $p < 0.01$. *Error bars*, S.D.

required for the specification of the most ventral neural progenitors (8, 9). GLI3 levels are low in the ventral neural tube. In E10.5 $Sltm^{-/-}$ neural tubes, V3 interneuron progenitor marker NKX2.2 levels were significantly reduced and OLIG2-expressing motor neuron progenitor regions were expanded (Fig. 8). This phenotype was seen in other mutant embryos that were defective in SHH signaling (36, 37). Together with our observations in $Sltm^{-/-}$ MEF and NIH3T3 cells, this result indicates that SLTM is important for GLI-dependent target gene expression and ventral neural tube progenitor specification.

SLTM enhances SHH-induced osteoblast differentiation

To determine whether SLTM functions in other SHH-dependent differentiation processes, we investigated the effect of excess SLTM on SHH-induced osteoblast differentiation of the mesenchymal stem cell-like C3H10T1/2 cells. SHH induces the differentiation of C3H10T1/2 cells into osteoblasts in a GLIA-dependent manner (38, 39). *Alp* is a direct target gene of GLI1/2 that is activated during differentiation (40). SHH treatment induced *Alp* expression in C3H10T1/2 cells, as shown by staining for alkaline phosphatase activities in plated cells (Fig. 9*A*). Overexpression of SLTM further enhanced SHH-induced *Alp* expression relative to levels in cells transfected with a control vector (Fig. 9*B*) and also significantly enhanced SHH-induced expression of *Gli1* and *Ptch1* (Fig. 9*B*). These results further confirmed that SLTM is a GLI regulator.

Discussion

In this study, using a newly generated $Gli3^{TAP}$ knock-in mouse and a proteomic approach, we found that SLTM interacts with GLI proteins to regulate SHH signaling bidirectionally. SLTM facilitates the binding of GLI3R to chromatin and enhances the repressor function of GLI3R. In the absence of GLI3R or when levels of GLI3R were low, SLTM increases the binding of GLIA to regulatory regions of SHH target genes and enhances GLIA-mediated gene activation and cell differentiation.

The $Gli3^{TAP}$ mouse we generated proved to be a useful tool to study GLI3 function. We first showed that the addition of the TAP tag did not significantly alter GLI3 activities. TAP-GLI3 protein was expressed and processed in a similar fashion as the WT GLI3. The $Gli3^{TAP/-}$ mice grow normally but have one extra first digit, a phenotype similar to $Gli3^{+/-}$ extra toe mice (30). The TAP tag allowed us to study the properties of endogenous GLI3. A similar tag knock-in mouse was generated to study GLI3 function (41). However, we believe that this study represents the first purification of endogenous GLI3-interacting complexes, which indicates the value of this mouse.

Using immunoprecipitation via the TAP tag, we identified SLTM as a novel GLI regulator. Our data indicate that SLTM interacts with GLI proteins in the nucleus and regulates the local and global binding of GLI proteins to chromatin. The exchange of the GLIR for GLIA transcription factors is a critical step in the production of SHH signaling outcomes. However, it was unknown how the binding of GLI proteins to target genes is regulated. It has been shown that nuclear GLI proteins are unstable after dissociation from SUFU (16, 21). Here, we demonstrated that SLTM plays an important role in regulating the balance between different GLI protein activities by differentially affecting their binding to chromatin. We showed that SLTM increased both GLI3R protein levels and GLI3 binding to chromatin. Because SLTM is a chromatin-associated protein that binds to GLI regulatory regions, we favor the scenario that SLTM stabilizes GLI3 proteins by interacting and retaining them on the chromatin. However, it is also possible that SLTM stabilizes GLI3, whereas increased GLI3 levels passively increased GLI3 binding to DNA. In the absence of GLI3, SLTM enhances GLIA activities, possibly through similar mechanisms.

As an important developmental signal, SHH signaling and transcription outcomes are precisely regulated. Interestingly, SHH signaling pathway components often play bidirectional roles, functioning as both activators and repressors of the pathway in a context-dependent manner. For example, the primary cilium is required for both GLI3R processes under basal conditions and for GLI1/2 activation in response to SHH (14, 42), and the chromatin-remodeling factor BRG1 is required for both repressing basal expression and for signaling-induced target gene expression (15, 27). Similarly, our data indicate that SLTM functions as a co-repressor of GLI3R under basal conditions, and in the absence of GLI3, SLTM functions as a co-activator of GLIA. Therefore, SLTM provides another level of precision in SHH signaling regulation.

The seemingly bidirectional function of SLTM in modulating GLIR and GLIA activities is regulated by SHH activities and GLI3R protein levels. SLTM facilitates GLI3 binding to target genes in cells under basal conditions. In response to SHH, SLTM protein levels decrease, which likely contributes to the departure of GLI3R from the target sites and reduction of

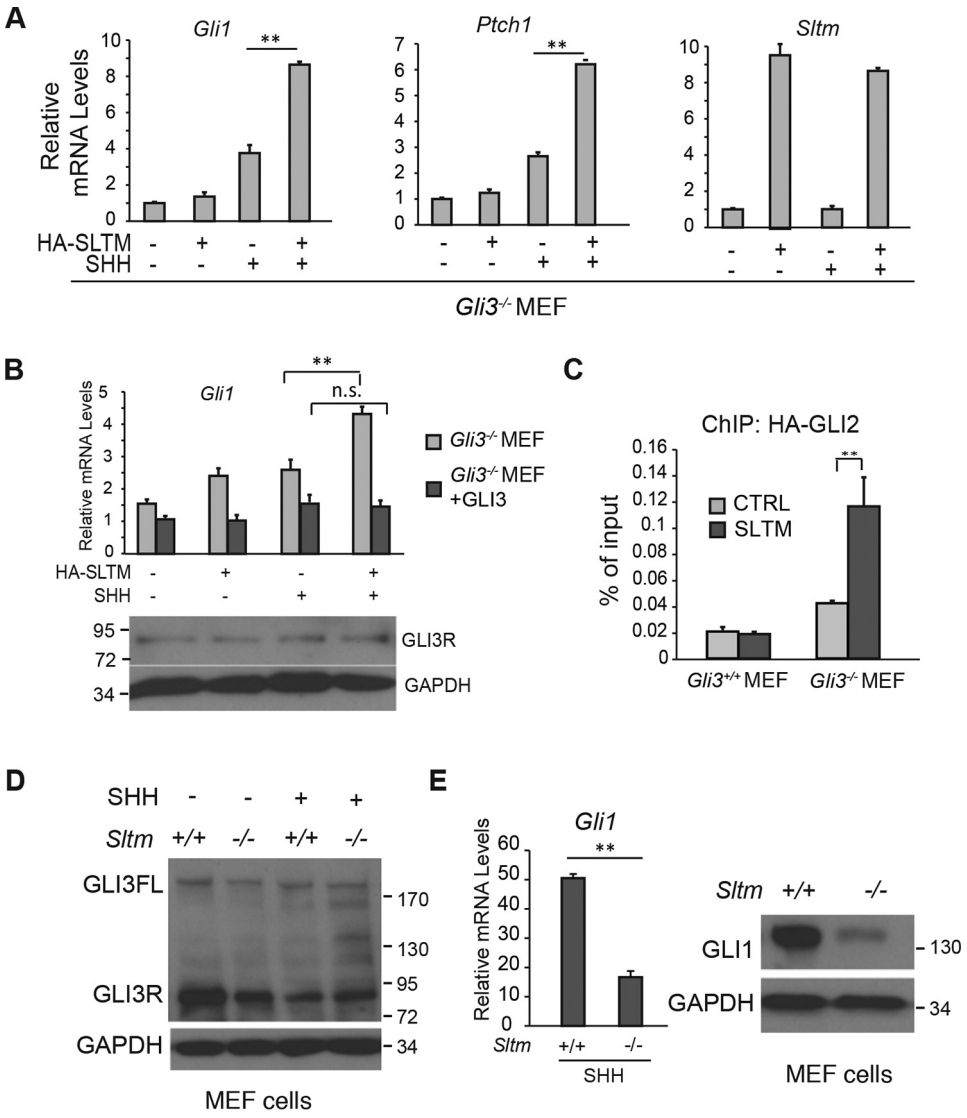

Figure 7. SLTM activates SHH/GLI target genes in the absence of GLI3R. *A*, SLTM activates expression of SHH/GLI target genes in *Gli3*$^{-/-}$ cells. RT-qPCR was used to analyze expression of *Gli1* and *Ptch1* in *Gli3*$^{-/-}$ MEFs transfected with a control or SLTM-expressing vector in the absence or presence of SHH. *B*, *Gli3*$^{-/-}$ cells were transfected with empty vector (*black*) or with a lentiviral construct for expression of GLI3R (*gray*), and the effects of SHH induction in the presence and absence of SLTM were evaluated. The presence of GLI3 diminished the activator functions of SLTM upon SHH treatment of cells. The *bottom panel* shows the exogenous GLI3R expression in *Gli3*$^{-/-}$ cells in each condition evaluated with Western blotting. *C*, ChIP-qPCR analysis of GLI2 binding to the *Gli1* regulatory region in WT or *Gli3*$^{-/-}$ cells expressing control (*gray*) or SLTM (*black*) indicates that GLI2 binding is enhanced by SLTM in the absence of GLI3. *D*, Western blotting was used to evaluate the levels of GLI3FL and GLI3R in WT and *Sltm*$^{-/-}$ MEFs in the presence and absence of SHH stimulation. *E*, GLI1 expression was evaluated in *Sltm*$^{-/-}$ MEFs and WT cells in the presence of SHH with RT-qPCR (graph) and Western blotting. qPCR graphics in *all panels* are representative of at least three experiments performed in triplicate ($n = 3$). Significance was determined by Student's *t* test or an ANOVA post hoc *t* test. **, $p < 0.01$. *Error bars*, S.D.

GLI3R levels. In SHH-stimulated cells in which SLTM was overexpressed, SLTM functioned as a co-repressor, possibly by increasing the amount of GLI3R bound to chromatin. In the absence of GLI3 (*e.g.* in *Gli3*$^{-/-}$ cells) or when GLI3 levels were relatively low (*e.g.* in SHH-stimulated cells or in *Sltm*$^{-/-}$ cells), SLTM enhanced GLIA binding and functioned as a co-activator of SHH target gene expression. Our data suggest that SLTM prefers to bind to GLI3R rather than GLIA in unstimulated NIH3T3/MEF cells (Fig. 3); the differential effects of SLTM on SHH target gene expression are likely due to this difference in binding affinity and to the relative amount of GLIA and GLIR in the cells. The SAFB proteins mainly serve as co-repressors. We found that SLTM overexpression led to a repressive chromatin environment in regulatory regions of SHH target genes. It is possible that SLTM recruits other co-repressors, such as PRC2, as a previously reported proteomic analysis demonstrated an interaction between PRC2 and SLTM (35). It is also possible that the increase of GLI3R binding to the enhancer region facilitated by SLTM indirectly results in a repressive chromatin environment. The fact that SLTM functions as a GLIA co-activator suggests, however, that SLTM-mediated effects on GLI protein binding to chromatin play a major role in determining the transcriptional outcomes.

SLTM is a member of the SAFB family proteins. Although it is less similar to the other two family members SAFB1 and SAFB2 than they are to each other (32, 33), it is not clear whether SAFB1 and SAFB2 compensate for the absence of SLTM *in vivo*. *Sltm*$^{-/-}$ MEF cells display defects in SHH target

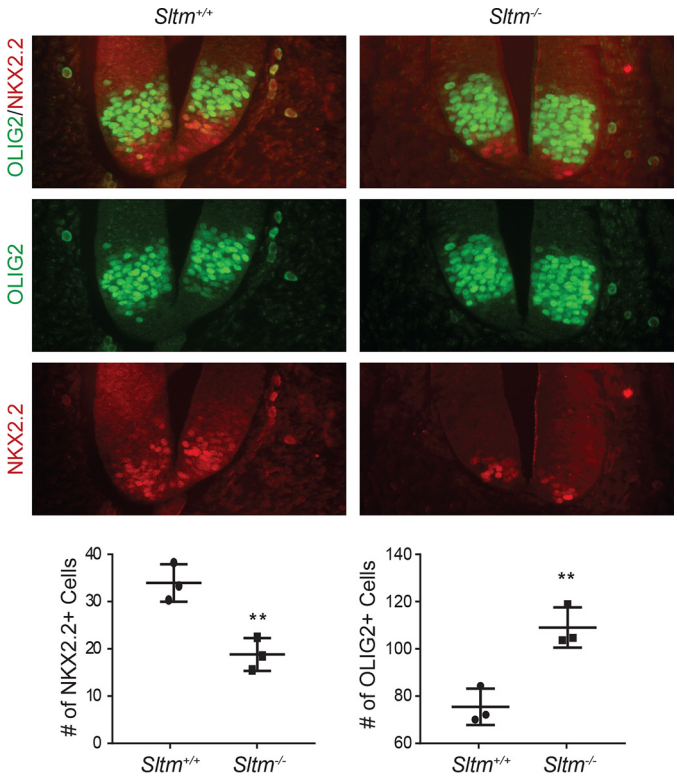

Figure 8. Abnormal expression of ventral neural tube markers in *Sltm*$^{-/-}$ embryos. Cross-sections of the mid-trunk neural tube regions of E10.5 WT and *Sltm*$^{-/-}$ embryos were stained with antibodies against ventral neural progenitor markers NKX2.2 (*red*) and OLIG2 (*green*). Representative overlay and single-channel pictures are shown. Reduction of NKX2.2-expressing cell numbers and the consequent expansion of OLIG2-expressing regions were quantified (the numbers are averages of positive cells in 15 sections from three pairs of WT and mutant embryos). Significance was determined by Student's *t* test. **, $p < 0.01$. *Error bars*, S.D.

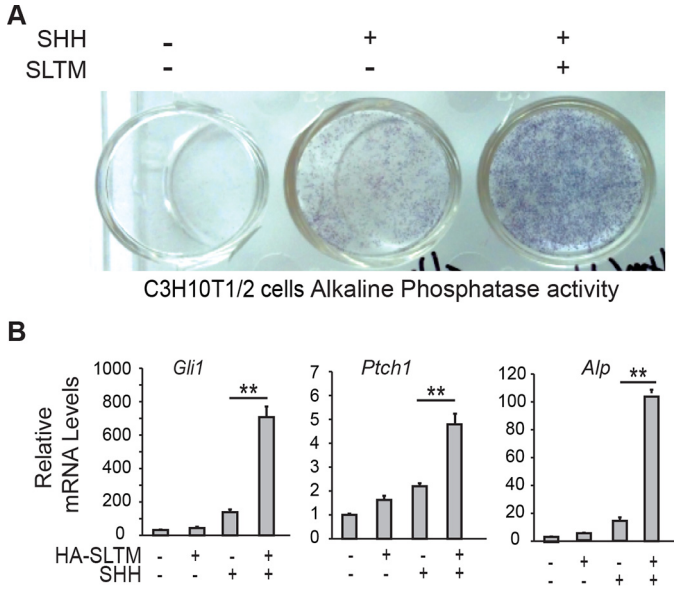

Figure 9. SLTM enhances SHH-induced C3H10T1/2 cell differentiation into osteoblasts. *A*, representative images of C3H10T1/2 cells treated with or without SHH for 7 days and with or without overexpression of SLTM. Cells were stained to reveal alkaline phosphatase activity indicative of differentiation. *B*, RT-qPCR was used to analyze SHH target gene expression in control and SLTM-expressing C3H10T1/3 cells treated with or without SHH for 7 days. RT-qPCR graphics are representative of at least three experiments performed in triplicate ($n = 3$). Significance was determined by an ANOVA post hoc *t* test. **, $p < 0.01$. *Error bars*, S.D.

gene expression under basal and SHH-induced conditions. *Sltm*-null embryos have defects in ventral neural tube, indicating its function in GLIA-mediated progenitor specification. However, *Sltm*-null mice did not display defects observed previously in *Gli3*$^{-/-}$ embryos (30). It is possible that other co-repressors such as SAFB family members, may have redundant functions *in vivo*. It is also possible that *Sltm* deletion led to impaired function of both GLIR and GLIA, which may rescue certain of the gross defects caused by GLIR deletion. These rescuing phenotypes were observed previously in *Shh/Gli3* and *Smo/Gli3* double knockouts (43–45). The positive function of SLTM in SHH-induced C3H10T1/2 osteoblast differentiation further suggests a physiological role of SLTM in the SHH-dependent developmental process.

In summary, we generated a *Gli3*^{TAP} knock-in mouse and used it to analyze GLI3 function. We performed a proteomic analysis of endogenous GLI3 complexes and identified SLTM as a novel regulator of GLI activities and SHH signaling outcomes. We uncovered a bidirectional function of SLTM; this protein can act as an activator or a repressor, depending on GLI3R levels. The function of SLTM in regulating GLI protein binding to chromatin was previously unknown, and this study revealed another layer of precise regulation of SHH signaling.

Experimental procedures

Generation of Gli3^{TAP} *knock-in mice*

Gli3^{TAP} knock-in mice were generated using homologous recombination. A bacterial artificial chromosome (RP22–256H21) containing the 5′ part of the *Gli3* gene (129S6/SvEvTac strain) was used to construct the knock-in template plasmid. The recombineering method was used to retrieve a 16.6-kb fragment flanking exon 2 (4.7 kb upstream and 11.6 kb downstream). A fragment encoding a TAP tag including both Protein A and HA tags was inserted immediately after the start codon of the *Gli3* gene. A Neo cassette flanked by two LoxP sites was inserted 0.3 kb downstream of the 3′ end of exon 2. The construct was transfected into SM-1 ES cells (129SvEv origin). Clones were digested with SacI and screened using Southern blotting using an outside probe (Fig. 1*C*). The upstream recombination was confirmed by PCR using a primer in the TAP tag and an outside primer (Fig. 1*B*). A clone containing the desired sequence was injected into C57/Bl6 blastocysts, which were used to generate chimeric mice. These mice were bred to C57/Bl6 mice to generate heterozygotes. To remove the Neo cassette, *Gli3*$^{TAP\text{-}neo}$ heterozygotes were crossed to *Nestin-Cre* transgenic mice (46), which express Cre in the germ cells. *Gli3*^{TAP} mice were bred to homozygotes, which display no obvious defects and are fertile. *Gli3*$^{+/-}$ mice (30) were kindly provided by Dr. J. Reiter (University of California, San Francisco, CA) and bred as a *Gli3*$^{+/-}$ intercross. All mice are maintained on a mixed genetic background at UT Southwestern Medical Center Animal Facility. All experiments in this study were approved by the institutional animal care and use committee at UT Southwestern Medical Center.

Generation of Sltm-null allele with the CRISPR/Cas9 method

RNA encoding Cas9 and guide RNA targeting exon 2 of *Sltm* were injected into pronuclei. The repair plasmid DNA contain-

ing the GFP-coding sequence and poly(A) signal was co-injected to generate the *Sltm*-null allele with GFP inserted in frame in exon 2. The region including exon 2 and flanking sequence was sequenced in the mice obtained. One progeny was obtained with GFP inserted correctly. The *Sltm*-null allele was genotyped by PCR using GFP1F (GCATGGACGAGCTGTACAAG) and Sltm1R (GTATCCCCATACCTTAAAACTTC) primers, and the WT allele was genotyped using Sltm2F (CCCCTTTCTGTGTAGCATAATTACTC) and Sltm2R (CCCCAGAATCAATAAAGAACTTTC) primers. $Sltm^{+/-}$ mice were crossed to generate $Sltm^{-/-}$ mice; the $Sltm^{-/-}$ mice died shortly after birth without obvious growth defects.

Affinity purification of TAP-GLI3 and MS analysis

Telencephalons from E13.5 WT or $Gli3^{TAP/TAP}$ embryos (30 embryos/sample) were homogenized in Buffer A (25 mM Tris, pH 7.5, 25 mM KCl, 5 mM $MgCl_2$, 10% glycerol, 0.1% NP-40, with protease inhibitor freshly added). The nuclei were washed once with Buffer A and then lysed with Purification Buffer (50 mM Tris, pH 8, 150 mM NaCl, 1% NP-40). The TAP tag was designed for tandem affinity purification with IgG followed by anti-HA antibodies. Due to the difficulty eluting GLI3 proteins by Tev digestion from several types of beads after the first purification step, we used a one-step affinity purification with IgG Sepharose 6 Fast Flow beads (GE Healthcare). Purification Buffer was used to wash the beads, and the same buffer with 1% SDS was used for elution. The eluted GLI3 complexes were run on SDS-polyacrylamide gels for a short distance. The total proteins were isolated and subjected for mass spectrophotometry analyses. Proteins from the gel slice were digested, extracted, and analyzed by LC/MS/MS using an Orbitrap Elite mass spectrometer (University of Texas Southwestern Proteomic Core Facility). Peptide identification was performed using the X!Tandem (47) and open MS search algorithm (OMSSA) search engines (48) against the mouse protein database from Uniprot. The precursor mass tolerance was 20 ppm, and the fragment mass tolerance was 0.5 Da. The false discovery rate was set to 0.01. Forty proteins that were only identified from the TAP-GLI3 samples and not from the control samples are listed in Table S1.

Generation of expression plasmids

The SLTM expression plasmid was obtained from Dr. Michael Norman (University of Bristol) (32). The *Sltm* coding region was cloned into the pSin-EF2 lentiviral vector to add the HA-Tag. GLI expression vectors and GLI3 fragments were described previously (15). GLI3N, GLI3 zinc finger, and GLI3C encode amino acids 1–425, 426–633, and 633–1580 of GLI3, respectively.

Cell culture and lentiviral infection

Primary $Sltm^{-/-}$ and control MEF cells were cultured from E13.5–E15.5 embryos. Briefly, embryo trunks were dissected, trypsinized, and dissociated to single cells. MEF cells were cultured in Dulbecco's modified Eagle's medium with 10% fetal bovine serum. Immortalized $Gli3^{-/-}$ MEF cells were provided by Dr. Wade Bushman (University of Wisconsin) (49). SHH conditioned medium was prepared as described previously (50). For SHH treatment, MEF cells or NIH3T3 cells were cultured in SHH-containing low-serum medium for 24 h. Lentiviruses were prepared according to a procedure described previously (51). PolyJet (Signagen) was used for plasmid transfection of cultured cells. Attached MEF cells were infected at an multiplicity of infection of 5 for 24 h with 8 μg/ml Polybrene.

Cell fractionation

Cell fractionation was performed as described (52). Briefly, NIH3T3 cells expressing exogenous SLTM were pelleted and resuspended in 10 mM Hepes, pH 7.9, 10 mM KCl, 1.5 mM $MgCl_2$, 0.34 M sucrose, 10% glycerol, 1 mM DTT. The supernatant was the cytoplasmic fraction, and the pellet was the nuclei. The nuclei were resuspended in 3 mM EDTA, 0.2 mM EGTA, 1 mM DTT. The pelleted chromatin fraction was resuspended in Laemmli buffer and sonicated prior to analysis.

Immunoblotting

For immunoblotting, cells or ground tissues were lysed in RIPA buffer (50 mM Tris, pH 8, 250 mM NaCl, 0.05% SDS, 0.5% deoxycholate, 1% NP-40). Histone fractions were prepared with acid extraction (0.2 N HCl). Cell lysates or histone fractions were separated on SDS-polyacrylamide gels. Antibodies used were against GLI1 (Cell Signaling), GLI3 (Roche Applied Science), SLTM (Bethyl Laboratory), GAPDH (Sigma), GFP (Clontech), HA (HA-7, Sigma), FLAG (M2, Sigma), and histone H3 (ab1791, Abcam). HRP-conjugated secondary antibodies were purchased from Jackson Immunology.

Immunohistology

Timed mouse pregnancies were determined by plugging date as day 0.5. Immunostaining was performed on paraffin sections. Antibodies used were against OLIG2 (Chemicon) and NKX2.2 (Developmental Studies Hybridoma Bank, University of Iowa). The images were visualized using an Olympus BX50 microscope. OLIG2- and NKX2.2-positive cells were counted from comparable sections of WT and *Sltm*-mutant neural tubes at the mid-trunk region. Averages of 15 sections from three embryos in each group (5 sections/embryo) were calculated and compared.

Co-immunoprecipitation experiments

Cells expressing tagged SLTM and tagged GLI proteins were lysed in Buffer A. Nuclear extracts were prepared in RIPA buffer (150 mM NaCl, 1.0% NP-40, 0.5% sodium deoxycholate, 0.1% SDS, and 50 mM Tris, pH 8.0) with rotation at 4 °C for 1 h. After centrifugation, antibodies against one tag were added to precleared nuclear extracts and incubated at 4 °C overnight. Samples were incubated with protein A beads (GE Healthcare) for 1 h; beads were washed with RIPA buffer four times. Precipitated proteins were eluted by boiling in 2× Sample Buffer before SDS-PAGE and Western blot analysis.

RT-PCR and qPCR

RNA from cells or ground tissues was extracted with TRIzol (Invitrogen). cDNAs were synthesized by reverse transcription with a blend of oligo(dT) and random primers using Iscript (Bio-Rad), followed by PCR or quantitative PCR analysis. A Bio-

Rad real-time PCR system (C1000 Thermal Cycler) was used for quantitative PCR. Levels of *GAPDH* mRNA were used to normalize input RNA. Graphics shown are representative of experiments performed in triplicate. The experiments were repeated at least three times. S.E. values were calculated according to a method described previously (15). Primers for ChIP-qPCR and RT-PCR were as follows: Gli1ChIP-P5F, CGTAACTGAGCTTTCCCCATGT; Gli1ChIP-P5R, CCTTCATGTTCCATAGGTCGC; ChIP-Ptch1F, GGACAGAGCATCTACCCTAAAAGA; ChIP-Ptch1R, TCAGTTCTTTAAGCTCCTGCACTA; ChIP-CD4F, CACCCTACGCTGACATAGTGGTTC; ChIP-CD4R, GCAAGATAGCTAAGCCAAACACATT; Ptch1F, GAAGCCACAGAAAACCCTGTC; Ptch1R, GCCGCAAGCCTTCTCTAGG; Gli1F, GGTCTCGGGGTCTCAAACTGC; Gli1R, CGGCTGACTGTGTAAGCAGAG.

ChIP

ChIP experiments were performed as described previously (15). Dounce-homogenized tissue or dissociated cells were cross-linked with paraformaldehyde or double-cross-linked with disuccinimidyl glutarate (Pierce) and sonicated into fragments of 200–500 bp. Antibodies used were against HA (Abcam), FLAG (Sigma), GLI3 (Roche Applied Science), H3K27me3 (EMD Millipore), SUZ12 (Cell Signaling), H3K9me2 (EMD Millipore), and histone H3 (ab1791, Abcam). Precipitated DNA was purified and subjected to real-time PCR.

Alkaline phosphatase activity assay

Alkaline phosphatase activity was determined as described previously (39). The C3H10T1/2 cells were washed with PBS, fixed with 3.7% formaldehyde, and stained with a mixture of 330 μg/ml nitro blue tetrazolium, 165 μg/ml bromochoroindoyl phosphate, 100 mM NaCl, 5 mM $MgCl_2$, and 100 mM Tris (pH 9.5).

Statistical analysis

At least three independent experiments were performed with each experiment analyzed in triplicate. Graphics shown are representative experiments. Data are expressed as means ± S.D. Statistical analysis was performed by either analysis of variance with ANOVA post hoc *t* test for multiple comparisons or a two-tailed unpaired Student's *t* test. A p value of <0.05 was considered significant.

Author contributions—Z. Z., X. Z., B. K., and J. W. designed and performed experiments and analyzed results. J. W. wrote the manuscript with help from all authors.

Acknowledgments—We are grateful to Drs. M. Norman, J. Reiter, J. Jiang, and W. Bushman for kindly providing reagents. We thank Qiu Wang and Ginger Zhou for technical help with mouse breeding. We also thank the Proteomic Core Facility and the Transgenic Core Facility (University of Texas Southwestern) for technical support.

References

1. Fuccillo, M., Joyner, A. L., and Fishell, G. (2006) Morphogen to mitogen: the multiple roles of hedgehog signalling in vertebrate neural development. *Nat. Rev. Neurosci.* **7,** 772–783 CrossRef Medline
2. Ingham, P. W., and McMahon, A. P. (2001) Hedgehog signaling in animal development: paradigms and principles. *Genes Dev.* **15,** 3059–3087 CrossRef Medline
3. Jiang, J., and Hui, C. C. (2008) Hedgehog signaling in development and cancer. *Dev. Cell* **15,** 801–812 CrossRef Medline
4. Briscoe, J., and Thérond, P. P. (2013) The mechanisms of Hedgehog signalling and its roles in development and disease. *Nat. Rev. Mol. Cell Biol.* **14,** 416–429 CrossRef Medline
5. Barakat, M. T., Humke, E. W., and Scott, M. P. (2010) Learning from Jekyll to control Hyde: Hedgehog signaling in development and cancer. *Trends Mol. Med.* **16,** 337–348 CrossRef Medline
6. Ingham, P. W., and Placzek, M. (2006) Orchestrating ontogenesis: variations on a theme by sonic hedgehog. *Nat. Rev. Genet.* **7,** 841–850 CrossRef Medline
7. Wang, B., Fallon, J. F., and Beachy, P. A. (2000) Hedgehog-regulated processing of Gli3 produces an anterior/posterior repressor gradient in the developing vertebrate limb. *Cell* **100,** 423–434 CrossRef Medline
8. Oosterveen, T., Kurdija, S., Alekseenko, Z., Uhde, C. W., Bergsland, M., Sandberg, M., Andersson, E., Dias, J. M., Muhr, J., and Ericson, J. (2012) Mechanistic differences in the transcriptional interpretation of local and long-range SHH morphogen signaling. *Dev. Cell* **23,** 1006–1019 CrossRef Medline
9. Peterson, K. A., Nishi, Y., Ma, W., Vedenko, A., Shokri, L., Zhang, X., McFarlane, M., Baizabal, J. M., Junker, J. P., van Oudenaarden, A., Mikkelsen, T., Bernstein, B. E., Bailey, T. L., Bulyk, M. L., Wong, W. H., and McMahon, A. P. (2012) Neural-specific Sox2 input and differential Gli-binding affinity provide context and positional information in SHH-directed neural patterning. *Genes Dev.* **26,** 2802–2816 CrossRef Medline
10. Aberger, F., and Ruiz I Altaba, A. (2014) Context-dependent signal integration by the GLI code: the oncogenic load, pathways, modifiers and implications for cancer therapy. *Semin. Cell Dev. Biol.* **33,** 93–104 CrossRef Medline
11. Pavletich, N. P., and Pabo, C. O. (1993) Crystal structure of a five-finger GLI-DNA complex: new perspectives on zinc fingers. *Science* **261,** 1701–1707 CrossRef Medline
12. Falkenstein, K. N., and Vokes, S. A. (2014) Transcriptional regulation of graded Hedgehog signaling. *Semin. Cell Dev. Biol.* **33,** 73–80 CrossRef Medline
13. Hui, C. C., and Angers, S. (2011) Gli proteins in development and disease. *Annu. Rev. Cell Dev. Biol.* **27,** 513–537 CrossRef Medline
14. Han, Y. G., Kim, H. J., Dlugosz, A. A., Ellison, D. W., Gilbertson, R. J., and Alvarez-Buylla, A. (2009) Dual and opposing roles of primary cilia in medulloblastoma development. *Nat. Med.* **15,** 1062–1065 CrossRef Medline
15. Zhan, X., Shi, X., Zhang, Z., Chen, Y., and Wu, J. I. (2011) Dual role of Brg chromatin remodeling factor in Sonic hedgehog signaling during neural development. *Proc. Natl. Acad. Sci. U.S.A.* **108,** 12758–12763 CrossRef Medline
16. Niewiadomski, P., Kong, J. H., Ahrends, R., Ma, Y., Humke, E. W., Khan, S., Teruel, M. N., Novitch, B. G., and Rohatgi, R. (2014) Gli protein activity is controlled by multisite phosphorylation in vertebrate Hedgehog signaling. *Cell Rep.* **6,** 168–181 CrossRef Medline
17. Tempé, D., Casas, M., Karaz, S., Blanchet-Tournier, M. F., and Concordet, J. P. (2006) Multisite protein kinase A and glycogen synthase kinase 3β phosphorylation leads to Gli3 ubiquitination by SCFbetaTrCP. *Mol. Cell. Biol.* **26,** 4316–4326 CrossRef Medline
18. Wang, B., and Li, Y. (2006) Evidence for the direct involvement of βTrCP in Gli3 protein processing. *Proc. Natl. Acad. Sci. U.S.A.* **103,** 33–38 CrossRef Medline
19. Chen, M. H., Wilson, C. W., Li, Y. J., Law, K. K., Lu, C. S., Gacayan, R., Zhang, X., Hui, C. C., and Chuang, P. T. (2009) Cilium-independent regulation of Gli protein function by Sufu in Hedgehog signaling is evolutionarily conserved. *Genes Dev.* **23,** 1910–1928 CrossRef Medline
20. Wang, C., Pan, Y., and Wang, B. (2010) Suppressor of fused and Spop regulate the stability, processing and function of Gli2 and Gli3 full-length activators but not their repressors. *Development* **137,** 2001–2009 CrossRef Medline

21. Humke, E. W., Dorn, K. V., Milenkovic, L., Scott, M. P., and Rohatgi, R. (2010) The output of Hedgehog signaling is controlled by the dynamic association between Suppressor of Fused and the Gli proteins. *Genes Dev.* **24,** 670–682 CrossRef Medline
22. Zhang, Y., Fu, L., Qi, X., Zhang, Z., Xia, Y., Jia, J., Jiang, J., Zhao, Y., and Wu, G. (2013) Structural insight into the mutual recognition and regulation between Suppressor of Fused and Gli/Ci. *Nat. Commun.* **4,** 2608 CrossRef Medline
23. Han, Y., Shi, Q., and Jiang, J. (2015) Multisite interaction with Sufu regulates Ci/Gli activity through distinct mechanisms in Hh signal transduction. *Proc. Natl. Acad. Sci. U.S.A.* **112,** 6383–6388 CrossRef Medline
24. Lin, C., Yao, E., Wang, K., Nozawa, Y., Shimizu, H., Johnson, J. R., Chen, J. N., Krogan, N. J., and Chuang, P. T. (2014) Regulation of Sufu activity by p66β and Mycbp provides new insight into vertebrate Hedgehog signaling. *Genes Dev.* **28,** 2547–2563 CrossRef Medline
25. Goetz, S. C., and Anderson, K. V. (2010) The primary cilium: a signalling centre during vertebrate development. *Nat. Rev. Genet.* **11,** 331–344 CrossRef Medline
26. Shi, X., Zhang, Z., Zhan, X., Cao, M., Satoh, T., Akira, S., Shpargel, K., Magnuson, T., Li, Q., Wang, R., Wang, C., Ge, K., and Wu, J. (2014) An epigenetic switch induced by SHH signalling regulates gene activation during development and medulloblastoma growth. *Nat. Commun.* **5,** 5425 CrossRef Medline
27. Jagani, Z., Mora-Blanco, E. L., Sansam, C. G., McKenna, E. S., Wilson, B., Chen, D., Klekota, J., Tamayo, P., Nguyen, P. T., Tolstorukov, M., Park, P. J., Cho, Y. J., Hsiao, K., Buonamici, S., Pomeroy, S. L., *et al.* (2010) Loss of the tumor suppressor Snf5 leads to aberrant activation of the Hedgehog-Gli pathway. *Nat. Med.* **16,** 1429–1433 CrossRef Medline
28. Dai, P., Akimaru, H., Tanaka, Y., Maekawa, T., Nakafuku, M., and Ishii, S. (1999) Sonic Hedgehog-induced activation of the Gli1 promoter is mediated by GLI3. *J. Biol. Chem.* **274,** 8143–8152 CrossRef Medline
29. Canettieri, G., Di Marcotullio, L., Greco, A., Coni, S., Antonucci, L., Infante, P., Pietrosanti, L., De Smaele, E., Ferretti, E., Miele, E., Pelloni, M., De Simone, G., Pedone, E. M., Gallinari, P., Giorgi, A., *et al.* (2010) Histone deacetylase and Cullin3-REN(KCTD11) ubiquitin ligase interplay regulates Hedgehog signalling through Gli acetylation. *Nat. Cell Biol.* **12,** 132–142 CrossRef Medline
30. Hui, C. C., and Joyner, A. L. (1993) A mouse model of Greig cephalopolysyndactyly syndrome: the extra-toesJ mutation contains an intragenic deletion of the Gli3 gene. *Nat. Genet.* **3,** 241–246 CrossRef Medline
31. Endoh-Yamagami, S., Evangelista, M., Wilson, D., Wen, X., Theunissen, J. W., Phamluong, K., Davis, M., Scales, S. J., Solloway, M. J., de Sauvage, F. J., and Peterson, A. S. (2009) The mammalian Cos2 homolog Kif7 plays an essential role in modulating Hh signal transduction during development. *Curr. Biol.* **19,** 1320–1326 CrossRef Medline
32. Chan, C. W., Lee, Y. B., Uney, J., Flynn, A., Tobias, J. H., and Norman, M. (2007) A novel member of the SAF (scaffold attachment factor)-box protein family inhibits gene expression and induces apoptosis. *Biochem. J.* **407,** 355–362 CrossRef Medline
33. Garee, J. P., and Oesterreich, S. (2010) SAFB1's multiple functions in biological control—lots still to be done! *J. Cell. Biochem.* **109,** 312–319 CrossRef Medline
34. Norman, M., Rivers, C., Lee, Y. B., Idris, J., and Uney, J. (2016) The increasing diversity of functions attributed to the SAFB family of RNA-/DNA-binding proteins. *Biochem. J.* **473,** 4271–4288 CrossRef Medline
35. Cao, Q., Wang, X., Zhao, M., Yang, R., Malik, R., Qiao, Y., Poliakov, A., Yocum, A. K., Li, Y., Chen, W., Cao, X., Jiang, X., Dahiya, A., Harris, C., Feng, F. Y., Kalantry, S., Qin, Z. S., Dhanasekaran, S. M., and Chinnaiyan, A. M. (2014) The central role of EED in the orchestration of polycomb group complexes. *Nat. Commun.* **5,** 3127 CrossRef Medline
36. Ding, Q., Motoyama, J., Gasca, S., Mo, R., Sasaki, H., Rossant, J., and Hui, C. C. (1998) Diminished Sonic hedgehog signaling and lack of floor plate differentiation in Gli2 mutant mice. *Development* **125,** 2533–2543 Medline
37. Balaskas, N., Ribeiro, A., Panovska, J., Dessaud, E., Sasai, N., Page, K. M., Briscoe, J., and Ribes, V. (2012) Gene regulatory logic for reading the Sonic Hedgehog signaling gradient in the vertebrate neural tube. *Cell* **148,** 273–284 CrossRef Medline
38. Yuasa, T., Kataoka, H., Kinto, N., Iwamoto, M., Enomoto-Iwamoto, M., Iemura, S., Ueno, N., Shibata, Y., Kurosawa, H., and Yamaguchi, A. (2002) Sonic hedgehog is involved in osteoblast differentiation by cooperating with BMP-2. *J. Cell. Physiol.* **193,** 225–232 CrossRef Medline
39. Shimoyama, A., Wada, M., Ikeda, F., Hata, K., Matsubara, T., Nifuji, A., Noda, M., Amano, K., Yamaguchi, A., Nishimura, R., and Yoneda, T. (2007) Ihh/Gli2 signaling promotes osteoblast differentiation by regulating Runx2 expression and function. *Mol. Biol. Cell* **18,** 2411–2418 CrossRef Medline
40. Hojo, H., Ohba, S., Yano, F., Saito, T., Ikeda, T., Nakajima, K., Komiyama, Y., Nakagata, N., Suzuki, K., Takato, T., Kawaguchi, H., and Chung, U. I. (2012) Gli1 protein participates in Hedgehog-mediated specification of osteoblast lineage during endochondral ossification. *J. Biol. Chem.* **287,** 17860–17869 CrossRef Medline
41. Lopez-Rios, J., Duchesne, A., Speziale, D., Andrey, G., Peterson, K. A., Germann, P., Unal, E., Liu, J., Floriot, S., Barbey, S., Gallard, Y., Müller-Gerbl, M., Courtney, A. D., Klopp, C., Rodriguez, S., *et al.* (2014) Attenuated sensing of SHH by Ptch1 underlies evolution of bovine limbs. *Nature* **511,** 46–51 CrossRef Medline
42. Tukachinsky, H., Lopez, L. V., and Salic, A. (2010) A mechanism for vertebrate Hedgehog signaling: recruitment to cilia and dissociation of SuFu-Gli protein complexes. *J. Cell Biol.* **191,** 415–428 CrossRef Medline
43. Litingtung, Y., and Chiang, C. (2000) Specification of ventral neuron types is mediated by an antagonistic interaction between SHH and Gli3. *Nat. Neurosci.* **3,** 979–985 CrossRef Medline
44. Wijgerde, M., McMahon, J. A., Rule, M., and McMahon, A. P. (2002) A direct requirement for Hedgehog signaling for normal specification of all ventral progenitor domains in the presumptive mammalian spinal cord. *Genes Dev.* **16,** 2849–2864 CrossRef Medline
45. Rallu, M., Machold, R., Gaiano, N., Corbin, J. G., McMahon, A. P., and Fishell, G. (2002) Dorsoventral patterning is established in the telencephalon of mutants lacking both Gli3 and Hedgehog signaling. *Development* **129,** 4963–4974 Medline
46. Tronche, F., Kellendonk, C., Kretz, O., Gass, P., Anlag, K., Orban, P. C., Bock, R., Klein, R., and Schütz, G. (1999) Disruption of the glucocorticoid receptor gene in the nervous system results in reduced anxiety. *Nat. Genet.* **23,** 99–103 CrossRef Medline
47. Craig, R., and Beavis, R. C. (2004) TANDEM: matching proteins with tandem mass spectra. *Bioinformatics* **20,** 1466–1467 CrossRef Medline
48. Geer, L. Y., Markey, S. P., Kowalak, J. A., Wagner, L., Xu, M., Maynard, D. M., Yang, X., Shi, W., and Bryant, S. H. (2004) Open mass spectrometry search algorithm. *J. Proteome Res.* **3,** 958–964 CrossRef Medline
49. Lipinski, R. J., Gipp, J. J., Zhang, J., Doles, J. D., and Bushman, W. (2006) Unique and complimentary activities of the Gli transcription factors in Hedgehog signaling. *Exp. Cell Res.* **312,** 1925–1938 CrossRef Medline
50. Chen, J. K., Taipale, J., Young, K. E., Maiti, T., and Beachy, P. A. (2002) Small molecule modulation of Smoothened activity. *Proc. Natl. Acad. Sci. U.S.A.* **99,** 14071–14076 CrossRef Medline
51. Tiscornia, G., Singer, O., and Verma, I. M. (2006) Production and purification of lentiviral vectors. *Nat. Protoc.* **1,** 241–245 CrossRef Medline
52. Méndez, J., and Stillman, B. (2000) Chromatin association of human origin recognition complex, cdc6, and minichromosome maintenance proteins during the cell cycle: assembly of prereplication complexes in late mitosis. *Mol. Cell. Biol.* **20,** 8602–8612 CrossRef Medline